

# The delay spread in fibers for SDM transmission: dependence on fiber parameters and perturbations

Cristian Antonelli,<sup>1,\*</sup> Antonio Mecozzi,<sup>1</sup> and Mark Shtaif,<sup>2</sup>

<sup>1</sup> Dept. of Physical and Chemical Sciences, University of L'Aquila, 67100 L'Aquila, Italy

<sup>2</sup> School of Electrical Engineering, Tel Aviv University, Tel Aviv, Israel 69978

[\\*cristian.antonelli@univaq.it](mailto:cristian.antonelli@univaq.it)

**Abstract:** Contrary to single mode fibers, where random imperfections are responsible for polarization-mode dispersion, modal dispersion (MD) in multi-mode fiber structures for space-division multiplexed (SDM) transmission, originates chiefly from the intrinsic non-degeneracy of the propagating modes, also known as modal birefringence. The presence of random imperfections in such fibers has a positive aspect, as it reduces the intrinsic MD, and in the limit of strong coupling it causes the signal delay spread to increase with the square root of the propagation distance, rather than linearly, as would be the case in an ideal fiber. In this paper we derive a formula that relates the signal delay spread to the fiber geometry and to the statistical properties of the structural fiber perturbations. The derived formula provides insight into the MD phenomenon and facilitates the design of low-MD multi-mode fiber structures.

© 2015 Optical Society of America

**OCIS codes:** (060.2330) Fiber optics communications; (060.4510) Optical communications; (060.4230) Multiplexing.

---

## References and links

1. H. Kogelnik and P.J. Winzer, "Modal birefringence in weakly guiding fibers," *J. Lightwave Technol.* **30**, 2240–2243 (2012).
2. C. Antonelli, A. Mecozzi, M. Shtaif, and P. J. Winzer, "Stokes-space analysis of modal dispersion in fibers with multiple mode transmission," *Opt. Express* **20**, 11718–11733 (2012).
3. K.-P. Ho and J.M Kahn, "Statistics of group delays in multi-mode fibers with strong mode coupling," *J. Lightwave Technol.* **29**, 3119–3128 (2011).
4. R. Ryf, R.-J. Essiambre, A. H. Gnauck, S. Randel, M. A. Mestre, C. Schmidt, P. J. Winzer, R. Delbue, P. Pupalaiakis, A. Sureka, T. Hayashi, T. Taru, and T. Sasaki, "SDM transmission over 4200-km 3-core microstructured fiber," *OFC 2011*, Paper PDP5C.2 (2011).
5. C. Antonelli, A. Mecozzi, M. Shtaif, and P. J. Winzer, "Random coupling between groups of degenerate fiber modes in mode multiplexed transmission," *Opt. Express* **21**, 9484–9490 (2013).
6. L. Palmieri, "Coupling mechanism in multimode fibers," *SPIE OPTO* (2013), Paper 90090G.
7. J.P. Gordon and H. Kogelnik, "PMD fundamentals: polarization mode dispersion in optical fibers," *Proc. Natl. Acad. Sci. USA* **97**, 4541–4550 (2000).
8. A. Mecozzi, C. Antonelli, and M. Shtaif, "Intensity impulse response of SDM links," to be published (2015).
9. C. Xia, N. Bai, I. Ozdur, X. Zhou, and G. Li "Supermodes for optical transmission," *Opt. Express* **19**, 16653–16664 (2011).
10. W. Snyder, "Coupled-mode theory for optical fibers," *J. Opt. Soc. Am.* **62**, 1267-1277 (1972).
11. A. Galtarossa and L. Palmieri, "Measure of twist-induced circular birefringence in long single-mode fibers: theory and experiments," *J. Lightwave Technol.* **20**, 1149–1159 (2002).

## 1. Introduction

One of the most critical challenges in space-division multiplexed (SDM) transmission over multi-mode and multi-core fibers is the fact that different fiber modes propagate with distinctively different velocities. This results in a significant delay spread, which constrains the complexity of the digital signal processing (DSP) required for the implementation of multiple-input multiple-output (MIMO) techniques. Unlike in the case of standard single-mode fibers, where the delay spread results from the presence of structural imperfections which produce random birefringence, in SDM fibers the delay spread is caused primarily by modal birefringence – an intrinsic property of multi-mode wave-guides, that exists even in ideal structures. Interestingly, in the multi-mode case, the existence of structural imperfections has a positive aspect. Indeed, in their presence, the temporal broadening of the transmitted waveforms is proportional to the *square root* of the system length, and not to the system length itself, as it would be in an ideal fiber [1]. While this is a well-known fact, pointed out in early SDM studies [2, 3] and verified experimentally [4], the relation between the various fiber parameters and the delay spread remains largely unknown. This relation is critical for the efficient design of SDM fibers with the scope of reducing the delay spread, and with it the requirements from the MIMO-DSP hardware.

In this paper we describe the mechanism which is responsible for the transition from a linear dependence of the temporal broadening on system length, which characterizes short fibers, to a square-root length dependence. In this sense, this paper generalizes our previous work [5], which focused only on the regime characterized by the linear length dependence. We derive a formula for the mean square length of the modal dispersion (MD) vector introduced in [2], which uniquely determines the signal delay spread. The formula that we derive applies to all types of SDM fibers, including multi-mode fiber (MMF) and multi-core fiber (MCF) structures, and accommodates perturbations having arbitrary statistical properties (indeed the characterization of the mechanisms that cause random mode coupling are a subject of ongoing research [6]). After introducing the general formula, we specialize it to the case of a three-core fiber of the kind used in [4] and exemplify its power in predicting the observed growth-rate of the delay spread with system length.

## 2. Problem setting and background

We consider an SDM fiber structure supporting  $2N$  modes, where  $N$  is the number of spatial modes and the factor of 2 accounts for polarization. We denote by  $\vec{E}$  the column vector whose components  $E_j(\omega)$  ( $j = 1 \dots 2N$ ) are the Fourier transforms of the complex envelopes of the electric field in the various modes. The linear evolution of the electric field in an SDM fiber is governed by the equation

$$\frac{\partial \vec{E}}{\partial z} = i\mathbf{B}\vec{E}, \quad (1)$$

where  $\mathbf{B}(\omega)$  is a  $2N \times 2N$  propagation matrix, which can be divided to three contributions  $\mathbf{B} = \beta\mathbf{I} + \mathbf{B}_0 + \mathbf{B}_n$ . Here  $\beta$  is the mode-averaged propagation constant,  $\mathbf{I}$  is the identity matrix,  $\mathbf{B}_0$  is a  $z$ -independent matrix accounting for differences in the deterministic propagation constants and for the deterministic mode coupling, whereas  $\mathbf{B}_n$  is a  $z$ -dependent matrix that accounts for random perturbations. In the absence of mode-dependent loss, and omitting the trivial contribution of mode-independent scattering losses (whose effect is immaterial to our study), the matrices  $\mathbf{B}_0$  and  $\mathbf{B}_n$  are Hermitian. In addition, since  $\beta$  accounts for the (immaterial) mode-averaged propagation constant,  $\mathbf{B}_0$  and  $\mathbf{B}_n$  are traceless.

$$\mathbf{B}_0 = \frac{\vec{b} \cdot \vec{\Lambda}}{2N}, \quad \mathbf{B}_n = \frac{\vec{n} \cdot \vec{\Lambda}}{2N}, \quad (2)$$

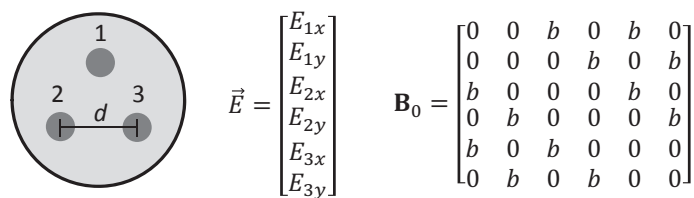


Fig. 1. On the left is the schematic of the three-core fiber that we assume in our examples. The fiber parameters are taken from [4]: each core's radius is  $r = 6.2 \mu\text{m}$ , the inter-core distance is  $d = 29.4 \mu\text{m}$ , and the refractive index difference between cores and cladding is of 0.27%. In the middle we show the structure of the Jones vector for this fiber in the reference frame of the individual cores. On the right we show the deterministic coupling matrix  $\mathbf{B}_0$ , where the coupling coefficient  $b$  can be obtained as in [10].

where  $\vec{\Lambda}$  is a vector whose  $D = 4N^2 - 1$  components are the generalized  $2N \times 2N$  Pauli matrices  $\Lambda_j$ , and where  $\vec{b}$  and  $\vec{n}$  are generalized birefringence vectors, representing the effects of the intrinsic fiber birefringence, and of the perturbations, respectively. Naturally  $\langle \vec{n} \rangle = 0$ , where the angled brackets denote statistical averaging. The  $D$  components of  $\vec{b}$  and  $\vec{n}$  can be extracted as  $b_j = \text{Trace}[\Lambda_j \mathbf{B}_0]$  and  $n_j = \text{Trace}[\Lambda_j \mathbf{B}_n]$ . In order to provide some intuition, we apply the above to the example of the three-core fiber ( $N = 3$ ) whose structure and propagation matrix  $\mathbf{B}_0$ , in the basis of the individual cores, are shown in Fig. 1. In this case, using the above recipe and the definition of the matrices  $\Lambda_j$  given in [2], one finds that  $\vec{b} = 2b\sqrt{N}(\hat{e}_{10} + \hat{e}_{16} + \hat{e}_{18} + \hat{e}_{24} + \hat{e}_{26} + \hat{e}_{32})$ , where  $\hat{e}_j$  ( $j = 1 \dots D$ ) is a unit vector corresponding to the  $j$ -th dimension of Stokes space.

Another key concept that is necessary for our analysis is modal dispersion, which is represented in Stokes space by the MD vector  $\vec{\tau}$ , also introduced in [2]. This vector is an extension of the polarization-mode dispersion (PMD) vector used in the analysis of single mode fibers [7], such that the principal states are the eigenvectors of the matrix  $\vec{\tau} \cdot \vec{\Lambda} / 2N$  and the delays are the corresponding eigenvalues. The MD vector uniquely determines the temporal broadening of the incident signal. This can be shown explicitly in two limiting cases; one where the principal states are constant across the signal bandwidth and another when they change rapidly within it. In the former case the delay spread  $T$  is defined as the difference between the largest and the smallest eigenvalues of  $\vec{\tau} \cdot \vec{\Lambda} / 2N$  [3, 2], and it is a random quantity whose mean square value is  $\langle T^2 \rangle = f^2(N) \langle \tau^2 \rangle$ , where  $f(N)$  is given in Eq. (3) of [2], and the angled brackets denote averaging over the ensemble of fibers. In the latter case, the delay spread  $T$  can be defined as the *temporal* root-mean square duration of the received pulse. It can be shown that in this case  $T$  is a deterministic quantity and it is equal to  $T^2 = \langle \tau^2 \rangle / 4N^2$  [8, 4]. In order to allow a comparison with the experiments reported in [4], we assume in what follows the second definition for the delay spread, while keeping in mind that the first definition is identical within a simple numerical scaling factor.

The evolution of the MD vector is governed by the equation

$$\frac{\partial \vec{\tau}}{\partial z} = \vec{b}_\omega + \vec{n}_\omega + (\vec{b} + \vec{n}) \times \vec{\tau}, \quad (3)$$

where the subscript denotes differentiation with respect to the angular frequency  $\omega$  and where the symbol  $\times$  denotes the generalized cross product between vectors [2]. The term  $\vec{n}_\omega$ , which accounts for the frequency dependence of the perturbations, contributes to the delay spread to a negligible extent as compared to the term  $\vec{b}_\omega$ , which accounts for the deterministic walk-off

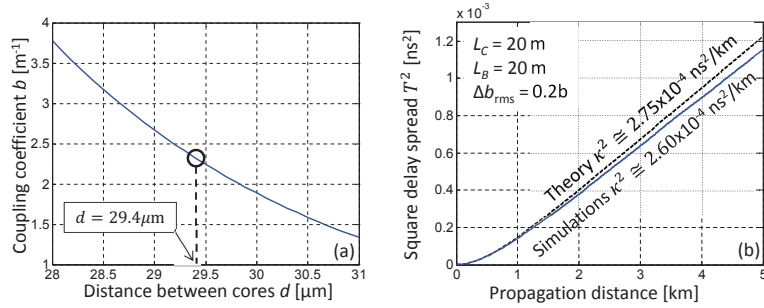


Fig. 2. a) The coupling coefficient  $b$  as a function of the inter-core distance  $d$ . Relative changes of  $b$  of the order of 20% can be seen to correspond to variations smaller than  $1\mu\text{m}$  in the inter-core distance. b) The square delay spread  $T^2$  versus distance for the displayed perturbation parameters. The solid curve shows the results of Monte Carlo simulations with  $10^4$  fiber realizations; the dashed curve is based on Eq. (4). The asymptotic growth-rate  $\kappa^2$ .

between non-degenerate modes. Therefore we neglect the contribution of  $\vec{n}_\omega$  in what follows. The final expression for  $T$  is provided below, while its derivation is deferred to Sec. 4.

### 3. Main results

Our main contribution in this Letter is in demonstrating that the delay spread  $T$  (which we define as  $T^2 = \langle \tau^2 \rangle / 4N^2$ ) associated with the propagation of  $2N$  modes, is given by

$$T^2 = \frac{2}{4N^2} \vec{b}_\omega \cdot \mathbf{Q}^{-1} [\mathbf{Q}^{-1} (\exp(\mathbf{Q}z) - \mathbf{I}) - \mathbf{I}z] \vec{b}_\omega \simeq \kappa z, \quad (4)$$

where the second equality holds in the limit of large  $z$ , with  $\kappa = \sqrt{-\vec{b}_\omega \cdot \mathbf{Q}^{-1} \vec{b}_\omega / 4N^2}$  being the *delay spread coefficient*. The expression for the matrix  $\mathbf{Q}$  is given by

$$\mathbf{Q} = \frac{1}{\Delta z} \int_{\Delta z} \exp(z' \vec{b} \times) \left\{ \sum_{i,j=1}^D \hat{e}_i \times \left[ \int_0^\infty N_{i,j}(\zeta) \exp(\zeta \vec{b} \times) d\zeta \hat{e}_j \right] \times \right\} \exp(-z' \vec{b} \times) dz', \quad (5)$$

where the external integration is performed over an interval of  $\Delta z$ , which is assumed to be much larger than the beat length between the nearest non-degenerate true fiber modes. In the example of a three-core fiber, the smallest beat length of the true modes, known in this case as supermodes [9], is  $2\pi/3b$ . The symbol  $(\vec{u} \times)$  is an operator that performs the generalized cross product, i.e.  $(\vec{u} \times) \vec{v} = \vec{u} \times \vec{v}$ , and it can be represented as a skew-symmetric  $D \times D$  matrix. The symbol  $N_{i,j}(\zeta)$  is the cross correlation function of the  $i$ -th and  $j$ -th components of the perturbation vector  $\vec{n}$ , namely  $N_{i,j}(\zeta) = \langle n_i(z + \zeta) n_j(z) \rangle$ .

We now apply Eq. (5) to our example of a three-core fiber, assuming the fiber parameters reported in [4]. We assume that perturbations are due to random and independent fluctuations in the three core-to-core distances, as well as due to random polarization coupling in the individual cores. The perturbations are therefore characterized by means of the standard deviation in the core-to-core distance and in terms of the beat length  $L_B$  between polarizations in the individual cores. The effect of fluctuations in the core-to-core distance  $d$  on the coupling coefficient  $b$  is summarized in Fig. 2a, which shows that changes of  $d$  smaller than  $1\mu\text{m}$  around the nominal value of  $29.4\mu\text{m}$  correspond to variations of the order of 20% in the value of  $b$ . We hence model these perturbations as independent complex circular Gaussian distributed fluctuations in

the coupling coefficients between each two cores with a standard deviation of  $\Delta b_{\text{rms}} = 0.2b$ . The coupling between polarizations within each individual core is modeled by means of a standard isotropically distributed birefringence vector, whose length is a Maxwellian random variable with a root-mean-square value of  $2\pi/L_B$ , as is customarily done in single-mode fibers [11]. With these assumptions one can construct the generalized birefringence perturbation vector  $\vec{n}$  as follows, using the definition of the matrices  $\Lambda_n$ ,  $n = 1 \dots 35$ , given in the appendix of [2]. All of its nonzero entries are independent Gaussian random variables, where the standard deviation  $\sigma_i$  of entries  $i \leq 9$  is  $2\pi/L_B$ , that of entries  $10 \leq i \leq 33$  is  $\sqrt{6}\Delta b_{\text{rms}}$ , whereas entries 34 and 35 are zero. Finally we assume that the perturbations decorrelate exponentially with a correlation length  $L_C$ , so that  $N_{i,j}(\zeta) = \delta_{ij}\sigma_i^2 \exp(-|\zeta|/L_C)$ , where  $\delta_{ij}$  is the Kronecker delta. Equation (5) therefore reduces to

$$\mathbf{Q} = \frac{1}{\Delta z} \int_{\Delta z} \exp(z'\vec{b} \times) \left\{ \sum_{i=1}^{35} \sigma_i^2 L_C \hat{e}_i \times \left[ \left( \mathbf{I} - L_C \vec{b} \times \right)^{-1} \hat{e}_i \right] \times \right\} \exp(-z'\vec{b} \times) dz'. \quad (6)$$

In Fig. 2b we plot the delay spread versus distance assuming  $L_B = 20\text{m}$  and  $L_C = 20\text{m}$ , which are typical values reported in studies conducted on single-mode fibers [11]. The solid curve shows the results of Monte Carlo simulations based on  $10^4$  fiber realizations, whereas the dashed curve is a plot of Eq. (4). The transition from weak to strong coupling between modes corresponds to the transition from the quadratic to linear dependence of  $T^2$  on the propagation distance. With this choice of the perturbation parameter values, a delay spread of approximately  $1\text{ns}^2$  for a system length of  $4000\text{km}$  is obtained, so as to reproduce the data reported in Fig. 2c of [4]. The value of  $\kappa$  extracted from simulations agrees with the theoretical value within an accuracy of about 97%.

In the table shown in Fig. 3 we report the values of the delay spread coefficient obtained from theory and simulations when varying one of the parameters  $b$ ,  $\Delta b_{\text{rms}}$ ,  $L_B$ , and  $L_C$ , relative to the configuration considered in Fig. 2, which is also shown in the first row of the table. The accuracy of the theoretical prediction is better than 94% in all cases. The second row of the table suggests that the delay spread coefficient increases with an increase in the coupling coefficient  $b$ . Indeed, an increase in  $b$  results in a larger value for  $|b_\omega|$  and hence in a larger walk-off between the supermodes of the three-core fiber. The third to fifth rows of the table suggest that the delay spread coefficient reduces when the fluctuations in the coupling coefficient  $\Delta b_{\text{rms}}$  (or, equivalently, in the inter-core distance) increase, or when the beat length  $L_B$  or the correlation length  $L_C$  reduce. We verified that these are not local trends, but rather they represent a general tendency in the dependence on these parameters. Indeed whenever  $\Delta b_{\text{rms}}$  increases, or when  $L_B$  or  $L_C$  decrease, the random mode coupling that is responsible for the transition from a linear dependence of the delay spread on  $z$  to a square-root dependence, becomes more substantial.

#### 4. Analysis

We start by applying the coordinate transformation  $\vec{\tau} = \exp\{z\vec{b} \times\} \vec{\tau}'$  to Eq. (3) where the term  $\vec{n}_\omega \times \vec{\tau}$  is omitted,

$$\frac{\partial \vec{\tau}'}{\partial z} = \exp\{-z\vec{b} \times\} \vec{b}_\omega + \vec{n}' \times \vec{\tau}', \quad (7)$$

so that  $\vec{n}' = \exp\{-z\vec{b} \times\} \vec{n}(z)$  is a new random process and  $|\vec{\tau}| = |\vec{\tau}'|$ . An important simplification in Eq. (7) is possible due to the fact that  $\vec{b} \times \vec{b}_\omega = 0$ , and hence  $\exp\{-z\vec{b} \times\} \vec{b}_\omega = \vec{b}_\omega$ . This can be seen in the reference frame of the true fiber modes, where  $\vec{b} \cdot \vec{\Lambda}$  and  $\vec{b}_\omega \cdot \vec{\Lambda}$  are diagonal matrices and hence they do commute. This leaves us with the equation

$$\frac{\partial \vec{\tau}'}{\partial z} = \vec{b}_\omega + \vec{n}' \times \vec{\tau}'. \quad (8)$$

$b$ [m <sup>-1</sup> ]	$\frac{\Delta b_{\text{rms}}}{b}$	$L_B$ [m]	$L_C$ [m]	$\kappa$ [ps/ $\sqrt{\text{km}}$ ] Simulations	$\kappa$ [ps/ $\sqrt{\text{km}}$ ] Theory	Accuracy
2.3	0.2	20	20	16.09	16.59	96.90%
2.74	0.2	20	20	18.74	19.32	96.91%
2.3	0.25	20	20	10.48	11.15	93.62%
2.3	0.2	5	20	13.27	13.90	95.29%
2.3	0.2	20	10	11.26	11.73	95.83%

Fig. 3. Theoretical and simulated values of the delay spread coefficient  $\kappa$  for various parameter settings. The first row coincides with the settings used in Fig. 2. In each of the rows from the second to the fifth only one parameter is varied.

Note that in the absence of perturbations, namely if  $\vec{n} = 0$ , Eq. (8) yields  $\vec{\tau}' = \vec{b}_\omega z$ , so that modal dispersion grows linearly with  $z$ . For this reason  $\vec{b}_\omega$  can be referred to as the *intrinsic birefringence vector* of the fiber [1]. In the general case, the equation for the mean square length of  $\vec{\tau}'$  is derived from Eq. (8), by using the property of the generalized vector product  $\vec{u} \cdot (\vec{u} \times \vec{v}) = 0$ , with the result

$$\frac{\partial \langle \tau'^2 \rangle}{\partial z} = 2 \left\langle \vec{\tau}' \cdot \frac{\partial \vec{\tau}'}{\partial z} \right\rangle = 2 \vec{b}_\omega \cdot \langle \vec{\tau}' \rangle. \quad (9)$$

which leaves us with the calculation of  $\langle \vec{\tau}' \rangle$ . To this end we first express  $\vec{\tau}'$  as a formal solution of Eq. (8),

$$\vec{\tau}'(z + \Delta z) = \vec{\tau}'(z) + \vec{b}_\omega \Delta z + \int_z^{z+\Delta z} \vec{n}'(z_1) \times \vec{\tau}'(z_1) dz_1. \quad (10)$$

We then use this expression iteratively in the evaluation of the increment  $\Delta \vec{\tau} = \vec{\tau}'(z + \Delta z) - \vec{\tau}'(z)$  from Eq. (8), and obtain

$$\Delta \vec{\tau}' = \vec{b}_\omega \Delta z + \Delta \vec{W} \times \vec{b}_\omega + \Delta \vec{W} \times \vec{\tau}'(z) + \int_z^{z+\Delta z} \int_z^{z'} \vec{n}'(z') \times \vec{n}'(z'') \times \vec{\tau}'(z'') dz'' dz', \quad (11)$$

where we defined the vectors  $\Delta \vec{W}$  and  $\Delta \vec{V}$  as follows,

$$\Delta \vec{W} = \int_z^{z+\Delta z} \vec{n}'(z') dz', \quad \Delta \vec{V} = \int_z^{z+\Delta z} (z' - z) \vec{n}'(z') dz'. \quad (12)$$

Note that no approximation was made in the derivation of (11) from (8). We now assume that the noise is small enough so as to produce small changes of the MD vector  $\vec{\tau}'$  in the interval  $\Delta z$ . Within this assumption we can replace  $\vec{\tau}'(z'')$  with  $\vec{\tau}'(z)$  in the double integral, and we can neglect the term  $\Delta \vec{V} \times \vec{b}_\omega$ , which is second order in  $\Delta z$ . Equation (11) simplifies to

$$\Delta \vec{\tau}' = \vec{b}_\omega \Delta z + \Delta \vec{W} \times \vec{\tau}'(z) + \mathbf{Q} \vec{\tau}'(z) \Delta z, \quad \mathbf{Q} = \frac{1}{\Delta z} \int_z^{z+\Delta z} \int_z^{z'} \vec{n}'(z') \times \vec{n}'(z'') \times dz'' dz'. \quad (13)$$

We now make the further assumption on the interval  $\Delta z$  being much greater than the correlation length of the perturbations  $L_C$ . It can be shown that the fluctuations of the matrix  $\mathbf{Q}$  are of the order of  $\Delta z$ , and hence, to zeroth order in  $\Delta z$ ,

$$\begin{aligned} \mathbf{Q} &\simeq \langle \mathbf{Q} \rangle = \frac{1}{\Delta z} \int_z^{z+\Delta z} \int_z^{z'} \left\langle \left[ \exp(-z' \vec{b} \times) \vec{n}(z') \right] \times \left[ \exp(-z'' \vec{b} \times) \vec{n}(z'') \right] \times \right\rangle dz'' dz' \\ &\simeq \frac{1}{\Delta z} \int_z^{z+\Delta z} \exp(z' \vec{b} \times) \left\{ \sum_{i,j=1}^D \hat{e}_i \times \left[ \int_0^\infty N_{i,j}(\zeta) \exp[\zeta \vec{b} \times] d\zeta \hat{e}_j \right] \times \right\} \exp(-z' \vec{b} \times) dz'. \end{aligned} \quad (14)$$

In the calculation of  $\langle \mathbf{Q} \rangle$  we expressed the perturbation vector in the original reference frame as  $\vec{n} = \sum_k^D n_k \hat{e}_k$ . The second line follows from the assumption that the correlation length of the perturbations is much shorter than the interval  $\Delta z$ , namely  $L_c \ll \Delta z$ , which allows extending the inner integral to the whole range of positive values of  $\zeta = z' - z''$ . It is important to note that the fast oscillations in the matrices  $\exp(\pm z' \vec{b} \times)$  are averaged out when integrating over several correlation lengths. In fact the nonzero eigenvalues of the matrix  $\vec{b} \times$  are imaginary and their inverse absolute value can be of the order of millimeters or centimeters, whereas correlation length values are estimated to be of the order of meters or tens of meters. This implies that  $\mathbf{Q}$  is independent of  $z$ . We verified that iterating the described procedure once more gives a second-order correction to the expression of  $\langle \tau^2 \rangle$  that notably improves the accuracy of the theory, thereby increasing the accuracies reported in the table of Fig. 3 up to 98% – 99%.

## 5. Conclusions

The delay spread in SDM fibers is caused mainly by the deterministic walk-off between the fiber modes. However, due to the random mode coupling caused by imperfections in the fiber structure, this delay spread does not accumulate linearly with propagation distance, as would be the case with ideal fibers. Rather, in the limit of strong coupling, which is always achieved asymptotically with the length of the link, it becomes proportional to the square root of the propagation distance. In this work we presented a formula that relates the root-mean-square delay spread to the main fiber parameters. Our results, when applied to the case of a three-core fiber, indicate that the delay spread coefficient decreases in the following cases: when the inter-core distances increases, when the magnitude of the fluctuations in the inter-core distance increases, and when the polarization beat length in the individual cores or the perturbations correlation length decreases.

## Acknowledgments

Discussions with Herwig Kogelnik and Peter J. Winzer are gratefully acknowledged. C. Antonelli and A. Mecozzi acknowledge financial support from the Italian Ministry of University and Research through ROAD-NGN project (PRIN2010-2011). M. Shtaif acknowledges financial support from Israel Science Foundation (grant 737/12) and the Terasanta consortium.